Electronic Supplementary Information

Ferroelectric enhanced Z-scheme P doped g-C_3N_4/PANI/$BaTiO_3$ ternary heterojunction with boosted visible-light photocatalytic water splitting

Qiannan Li,[†] Yuguo Xia,*[,‡] Kangliang Wei,[†] Xiaotong Ding,[†] Shun Dong,[‡] Xiuling Jiao*[,†], Dairong Chen[†‡]

[†]*School of Chemistry & Chemical Engineering, Shandong University, Jinan 250100, P. R. China*

[‡]*National Engineering Research Center for Colloidal Materials, Shandong University, Jinan 250100, P. R. China*

***Theoretical calculation*.** To better understand the electronic transfer mechanism involved in the interfaces of photocatalysts, spin-polarized density functional theory calculations were carried out with the Perdew-Burke-Ernzenhof (PBE) exchange correlation functional[1] and projector-augmented wave (PAW) pseudopotentials[2] as implemented in the Vienna ab initio simulation package (VASP)[3,4] The wave functions were expanded in a plane wave basis with an energy cutoff of 500 eV. The gamma centered scheme K-points grid sampling was set at Γ point for all the calculations. The van der Waals (vdW) interactions were involved which were corrected by the DFT-D3 approach[5] and all the structural relaxations were carried out until the residual forces were below 0.02 eV $Å^{-1}$. To obtain exact band gaps of PCN and PCN/PANI heterostructure, Heyd-Scuseria-Ernzerhof (HSE) hybrid functional with ω equals to 0.2 $Å^{-1}$ was employed. [6]

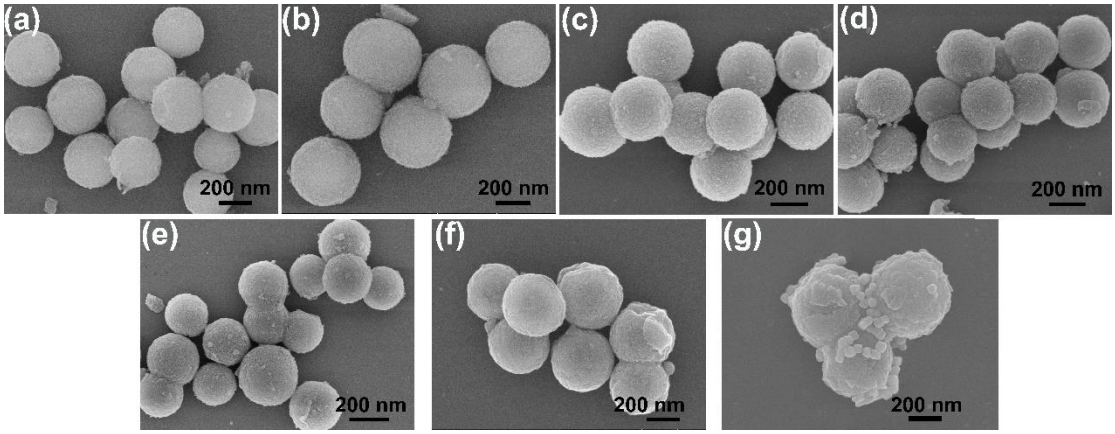

Fig. S1. SEM images for the morphology evolution in the synthetic process.

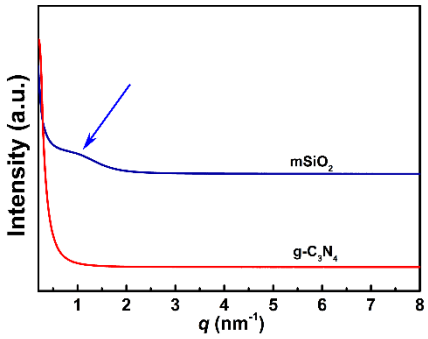

Fig. S2. SAXS patterns of mesoporous SiO_2 and g-C_3N_4.

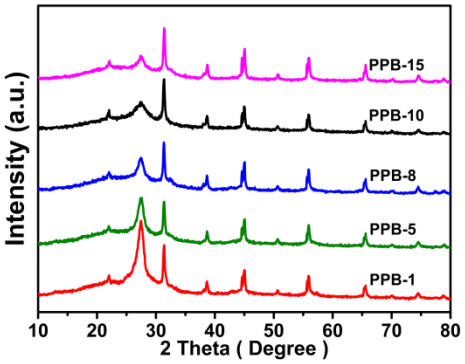

Fig. S3. XRD patterns of the PPB-*x* samples.

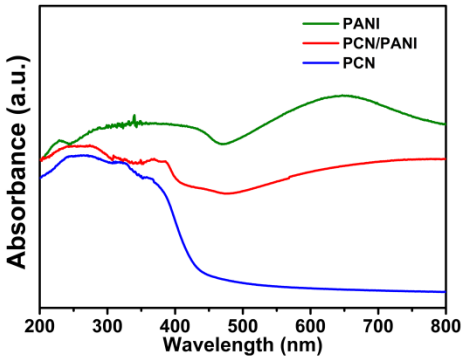

Fig. S4. UV-vis diffuse reflectance spectroscopy of PCN, PANI and PCN/PANI.

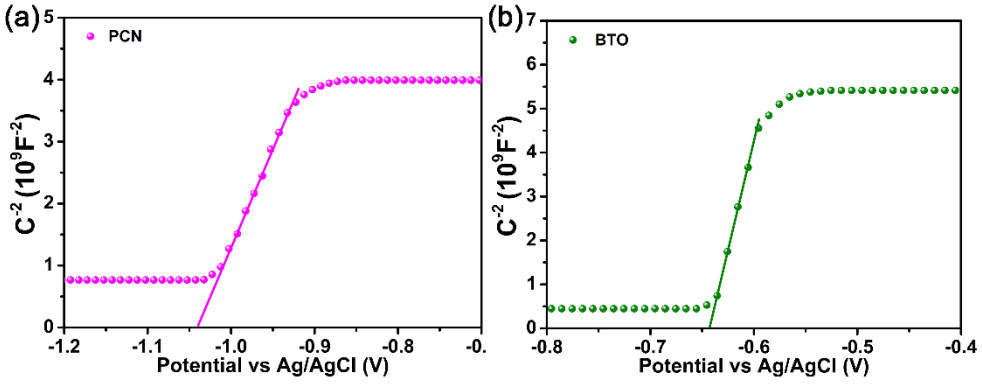

Fig. S5. Mott-Schottky plots for PCN and BTO.

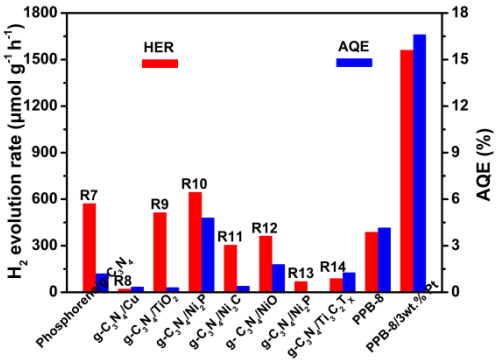

Fig. S6. Comparison of H_2 generation and AQE with that reported for other up-to-date g-C_3N_4 based photocatalysts at 420 nm.

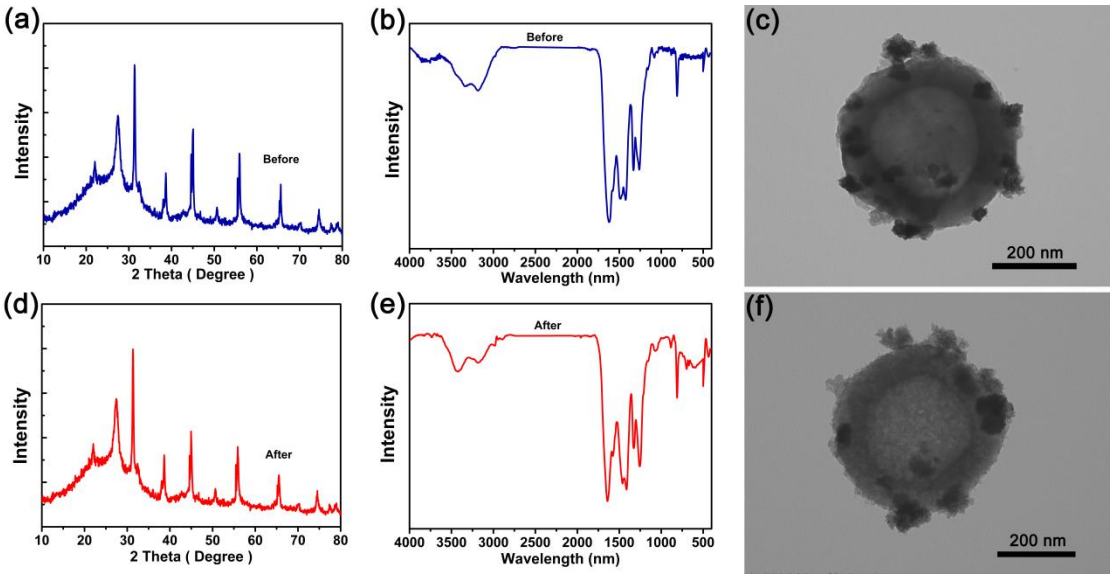

Fig. S7. Comparison of XRD, FT-IR and TEM of pristine PPB-8 photocatalyst and sample after six consecutive recycling experiments.

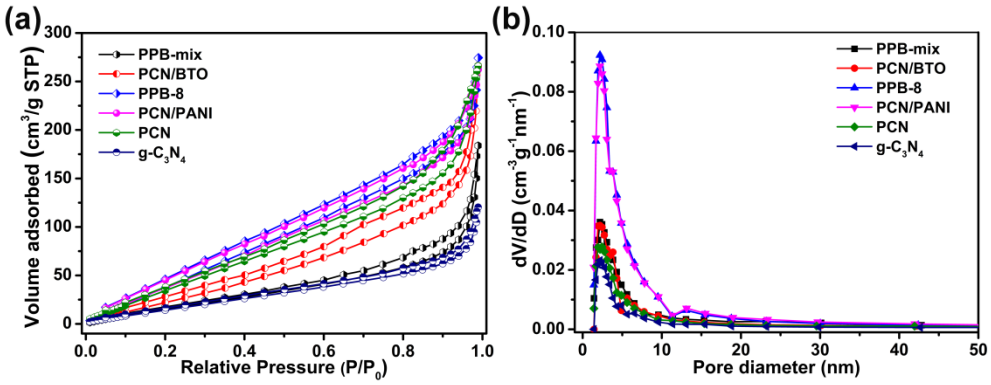

Fig. S8. (a) Nitrogen adsorption-desorption isotherms and (b) pore size distribution curve.

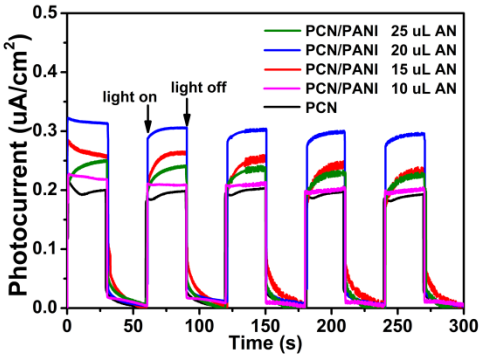

Fig. S9. Effect of loading amount of PANI on photocurrent.

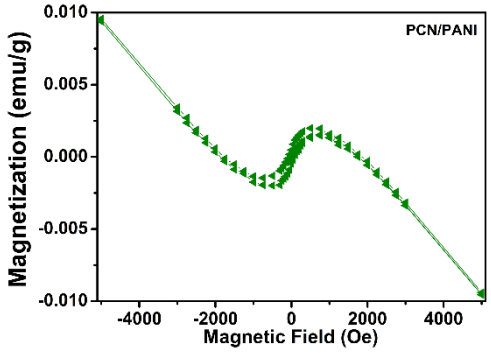

Fig. S10. Room temperature magnetic hysteresis loops of PCN/PANI.

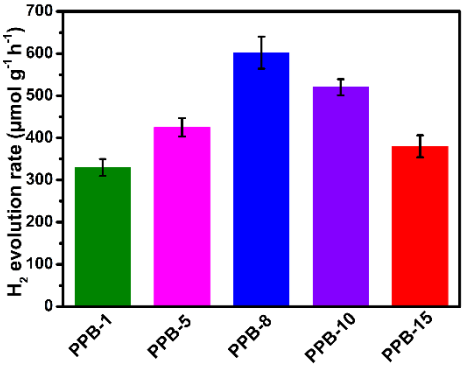

Fig. S11. Effect of loading amount of BTO on hydrogen evolution rate.

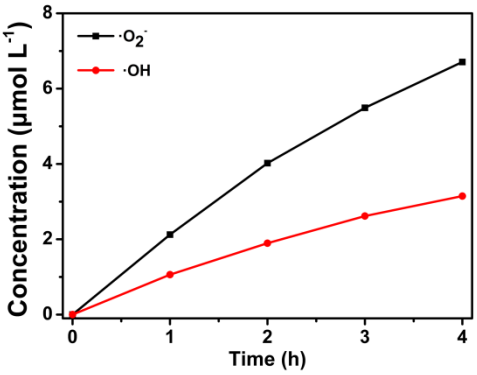

Fig. S12. Quantitative determination of generated $\bullet O_2^-$ and •OH for PPB.

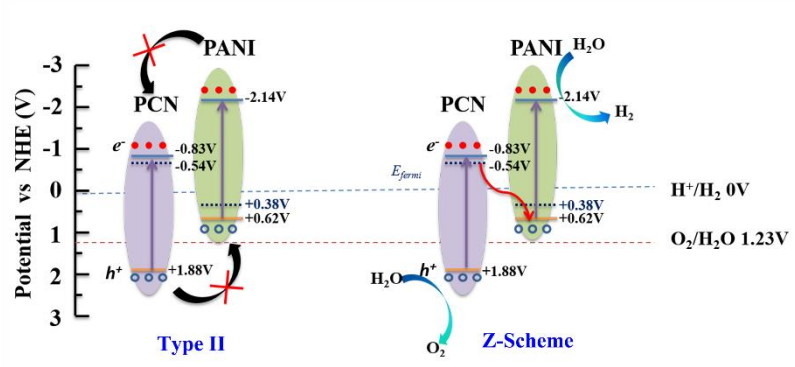

Fig.S13. Schematic diagram for photoinduced electron and hole transfer route in PCN/PANI junction.

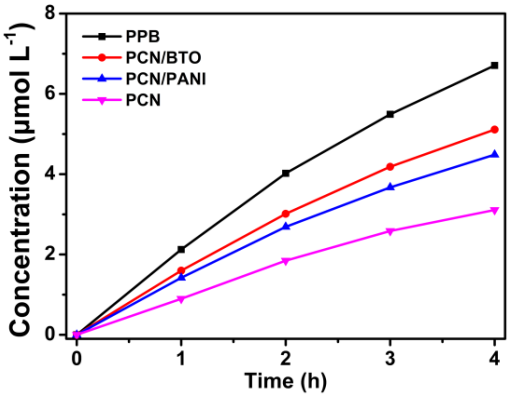

Fig. S14. Trapping rate comparison for PCN, PCN/PANI, PCN/BTO and PPB.

Table S1. Pore structure parameters obtained from the nitrogen desorption isotherm.

Sample	S_{bet}/(m^2/g)	V_{Tot}/(cm^3 g^{-1})	D_{av}/ (nm)
g-C_3N_4	86	0.157	9.1
PCN	119	0.186	8.7
PCN/PANI	129	0.406	6.3
PPB-8	132	0.428	6.0
PCN/BTO	111	0.231	10.1
PPB-mix	98	0.224	7.5

Table S2. Physicochemical data of PPB-*x*.

Sample	BTO/(PPB) wt.%	Nanoparticle size nm	BET m^2 g^{-1}	Pore volume cm^3 g^{-1}	Eg eV	HER umol g^{-1} h^{-1}
PPB-1	1	40 ± 3	122	0.412	2.52	329
PPB-5	5	40 ± 3	138	0.436	2.51	424
PPB-8	8	40 ± 3	132	0.428	2.51	602
PPB-10	10	40 ± 3	128	0.342	2.51	520
PPB-15	15	40 ± 3	120	0.297	2.50	380

References

1 J. Heyd, G. E. Scuseria, M. Ernzerhof, J.Chem.Phys. 2003, 118, 8207.

2 J. P. Perdew, K. Burke, M. Ernzerhof, Phys.Rev.Lett. 1996, 77, 3865.

3 P. E. Blöchl, Phys.Rev.B 1994, 50, 17953.

4 G. Kresse, J. Furthmüller, Comp.Mater.Sci. 1996, 6, 15.

5 G. Kresse, J. Hafner, Phys. Rev. B 1993, 47, 558.

6 S. Grimme, J. Antony, S. Ehrlich, H. Krieg, J.Chem.Phys. 2010, 132, 154104.

7 J. Ran, W. Guo, H. Wang, B. Zhu, J. Yu, S. Z. Qiao, *Adv. Mater.,* 2018, **30**, 1800128.

8 M. S. Fan, C. J. Song, T. J. Chen, X. Yan, D. B. Xu, W. Gu, W. D. Shi, L. S. Xiao, *RSC Adv.,* 2016**, 6**, 34633-34640.

8 Y. G. Tan, Z. Shu, J. Zhou, T. T. Li, W. B. Wang, Z. L. Zhao, *Appl. Catal., B,* 2018, **230**, 260-268

10 A. Indra, A. Acharjya, P. W. Menezes, C. Merschjann, D. Hollmann, M. Schwarze, M. Aktas, A. Friedrich, S. Lochbrunner, A. Thomas, M. Driess, *Angew. Chem., Int. Ed.,* 2017, **56** , 1653-1657.

11 K. L. He, J. Xie, Z.-Q. Liu, N. Li, X. B. Chen, J. Hu, X. Li, *J. Mater. Chem. A,* 2018, **6**, 13110-13122.

12 W. J. Wang, T. C. An, G. Y. Li, D. H. Xia, H. J. Zhao, J. C. Yu, P. K. Wong, *Appl. Catal., B,* 2017, **217**, 570-580.

13 J. N. Liu, Q. H. Jia, J. L. Long, X. X. Wang, Z. W. Gao, Q. Gu, *Appl. Catal., B,* 2018, **222**, 35-43.

14 Y. L. Sun, D. Jin, Y. Sun, X. Meng, Y. Gao, Y. Dall'Agnese, G. Chen, X.-F. Wang, *J. Mater. Chem. A,* 2018, **6**, 9124-9131.